International Journal of Engineering Technology and Scientific Innovation

ISSN: 2456-1851

Volume: 04, Issue: 05 "September-October 2019"

REAL-TIME IMPLEMENTATION OF MONITOR ALGORITHM ON AN ARM MICROPROCESSOR TO BE USED AS A WEARABLE VIBROTACTILE AID

Parivash Ranjbar[1,2], Amin Saremi[3], Dag Stranneby[4]

[1]Audiological Research Center at Örebro, University Hospital at Örebro, Sweden

[2]School of Health Sciences, Örebro University, Örebro, Sweden.

[3]Hearing4all and Department of Computational Neuroscience,
Carl von Ossietzky University of Oldenburg, Oldenburg, Germany

[4]School of Science and Technology s, Örebro University, Örebro, Sweden.

ABSTRACT

Individuals with combined severe hearing and visual impairment mainly rely on their skin sense to get information about environmental sounds. A multichannel algorithm, 'MONITOR', consisting of six filters and sinusoidal modulators, was devised to convert auditive sounds into tangible vibrations. This paper presents a real-time implementation of this algorithm on an ARM Cortex-M4 digital signal processor (DSP). The implemented system comprises an input pre-processing stage that captures, enhances and filters the incoming sounds which are then sampled, buffered and digitally processed by the DSP where MONITOR and a simple noise management algorithm are applied; the result is sent to the DSP's digital-to-analog convertor (DAC) and is sufficiently amplified to drive the vibrotactile transducer placed on the wrist. The results show that the system codes a large intensity range (40 to 94 dB SPL) and a broad frequency band of input sounds (0.1 to 6 kHz) and delivers approximately 4.3 [m/s2] mechanical acceleration in response to a 1 kHz sinusoid input at 94 dB SPL, which can be vividly sensed on the human wrist.

The presented DSP-based implementation manifests some important advantages over an existing mobile-based implementation of this algorithm, and is suitable for being produced as a wearable biomedical device.

Keywords: Deafblindness, Deafness, Vibration, Environmental sound, Vibrotactile aid, ARM cortex-M4, DSP

ISSN: 2456-1851

Volume: 04, Issue: 05 "September-October 2019"

1. INTRODUCTION

Persons with profound hearing impairment, and especially those with deafblindness, receive limited information about the surrounding world and mainly rely on their vibrotactile sensation to detect and identify events in their surroundings [1]. Borg et al. [1] examined 19 subjects with dual sensory impairments (hearing and vision) and found out that they actively use the vibratory information cues to perceive the ongoing events in the surrounding environment.

Besides of alarms, phone and doorbell chimes, one of the important and most information-rich environmental sounds is speech. The contribution of vibratory cues to the understanding of speech has been extensively studied [2] and several vibratory aids [2, 3] have been produced to convert speech information to vibrotactile signals for profoundly hearing impaired persons. One of these vibratory aids, Sentiphone MiniVib4, could substantially decrease the word error rate from 24% down to just 3.3% when added to normal visual lip-reading (i.e. speechreading) [3]. This type of vibratory aid can therefore result in a remarkable benefit in speech perception for post-lingual users that have some residual vision sensation. Users of this device also showed much better awareness of their environment and better control of their own voice when talking [4].

MiniVib4 signal processing is based on a single band-pass filter (bandwidth: 500 Hz to 2300 Hz) and amplitude modulation by a 220 Hz sinusoid [3]. Ranjbar et al. [5] expanded this method to form the amplitude-modulated multi-channel (AMMC) signal processing algorithm that enables a wider bandwidth. The algorithm, which is hereafter called 'MONITOR' and is depicted in Fig.7 of [5], consists of six channels. Each channel comprises a band-pass filter whose output envelope is amplitude-modulated by a specific sinusoid and then all results are summed up and sent to a vibrator. Ranjbar et al. [5] compared their MONITOR algorithm with 5 other algorithms, including MiniVib4, using some 45 pre-recorded environmental sounds (events) and found that MONITOR enables better identification of those events.

This work presents a real-time implementation of the MONITOR algorithm, shown in Fig. 1(A), on a digital signal processing (DSP) platform. The human skin consists of four different mechanoreceptors [6] and its vibratory sensation threshold is not only frequency-dependent but also depends on many other factors such as the diameter of the vibrating probe and the gap junction between the probe and the surrounding body of the vibrator [7]. In this implementation, a vibrator with 8-mm probe and a gap junction of about 2mm was used. Oey and Mellert [7] used a similar vibrator and showed that the skin codes frequencies typically between 75 Hz and 400 Hz with the highest sensitivity at around 200 Hz. The modulation sinusoids in the original

ISSN: 2456-1851

Volume: 04, Issue: 05 "September-October 2019"

MONITOR algorithm [5] were therefore adjusted to 75, 140, 205, 270, 335, and 400 Hz to cover the frequency range measured by Oey and Mellert [7] with a similar vibrator.

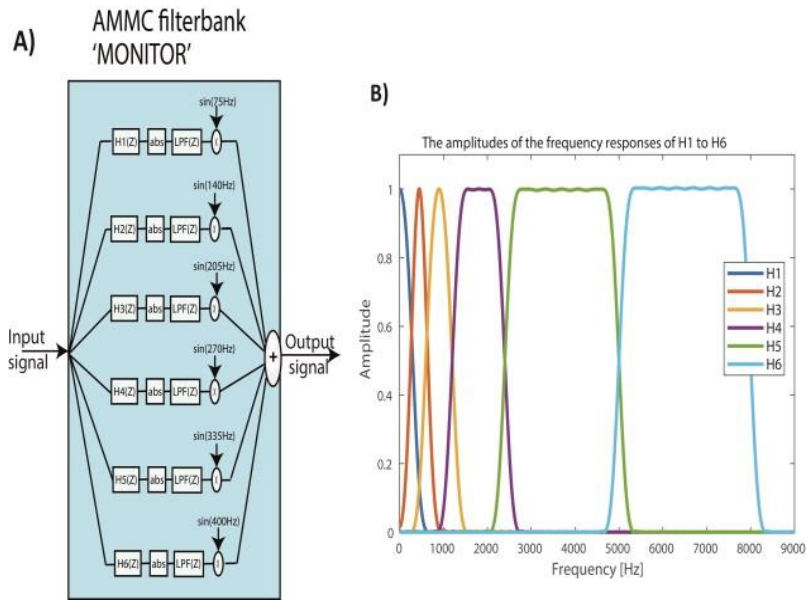

Fig. 1: A) The amplitude-modulated multichannel (AMMC) filterbank called 'MONITOR' which consists of 6 band-pass filters (H1 to H6), a low-pass filter (LPF), and 6 sinusoidal modulators. B) The amplitudes of the frequency responses for the band-pass filters H1 to H6.

Fig. 1(A) illustrates a description of the MONITOR algorithm. H1 to H6 are all band-pass filters with the following cutoff frequencies in Hz, respectively: H1: 0-300, H2: 300-600, H3: 600-1200, H4: 1200-2400, H5: 2400-5000, and H6:5000-8000. In this work, finite impulse response (FIR) filters of order 127 were used for the band-pass filters. Fig. 1(B) shows the amplitudes of the frequency responses for H1 to H6. The low-pass filter (LPF) was implemented by a 3rd order FIR filter with the cutoff frequency at 200 Hz.

Ranjbar and Stenstörm [8] implemented the MONITOR algorithm as a mobile application. The DSP-based implementation presented in this paper exhibits some important advantages over this mobile-based implementation as well as over the MiniVib4 solution [3]. These advantages are described and investigated in the discussion section of the paper.

2. METHODS

2.1 Material

ISSN: 2456-1851

Volume: 04, Issue: 05 "September-October 2019"

A microphone module with an omni-directional microphone component based on micro electro-mechanical systems (MEMS) technology was used as the input sensor. The captured signal was biased and adjusted using an operational amplifier. The MONITOR algorithm was digitally implemented on a 32-bit Cortex M4, ARM-based STM32F429 microprocessor provided in form of a discovery board by STelectronics [9] using Keil uVision integrated development environment (IDE). Keil uVison includes a compiler that compiles the C code written in this project into the binaries tailored to this specific microprocessor. Cortex M4 ARM microprocessors (such as STM32F429) are equipped with floating-point unit (FPU) and support DSP instructions. STM32F429 includes several internal 12-bit analog-to-digital convertor (ADC) and DAC channels. Its central computing processor's (CPU) computational power has scored 225 Dhrystone million instructions per second (MIPS), clocked at 180 MHz [9].

This microprocessor is also equipped with a direct memory access (DMA) unit that runs on an independent clock from that of the CPU, which is a vital feature for real-time implementations and the continuous input-to-output flow of the data [10]. The vibrator is a 7-ohm wearable miniature vibrotactile transducer that consists of a circular 2-mm vibrating metal plate that is placed with a 2-mm gap from the main body. The vibrator can convert electrical signals from 50 Hz to 400 Hz into mechanical vibrations but has its best sensitivity at 150-250 Hz. The vibrations generated at the output of the system were measured by a Brüel & Kjær type 4371 charge accelerometer connected via a low-noise rod to a standard oscilloscope.

2.2 Analog Input Pre-Processing Stage

Fig. 2(A) shows the input stage of the system. The operational amplifier UA1 acts as a 'buffer' between the microphone module and the microprocessor. UA1 is biased in inverting mode and amplifies the signal by R2/R1 ratio. This ratio is set to 33 so that the signal reaches its maximum peak-to-peak value (3.6V) in response to a 94 dB SPL tone, marking the upper end of the system's dynamic range. Furthermore, C1, R1, and R2 create an active first-order low-pass filter according to (1) below, where A_v is the gain.

$$A_v = \frac{R_2}{R_1 C_1 \times 2\pi \times f + R_1} (1)$$

ISSN: 2456-1851

Volume: 04, Issue: 05 "September-October 2019"

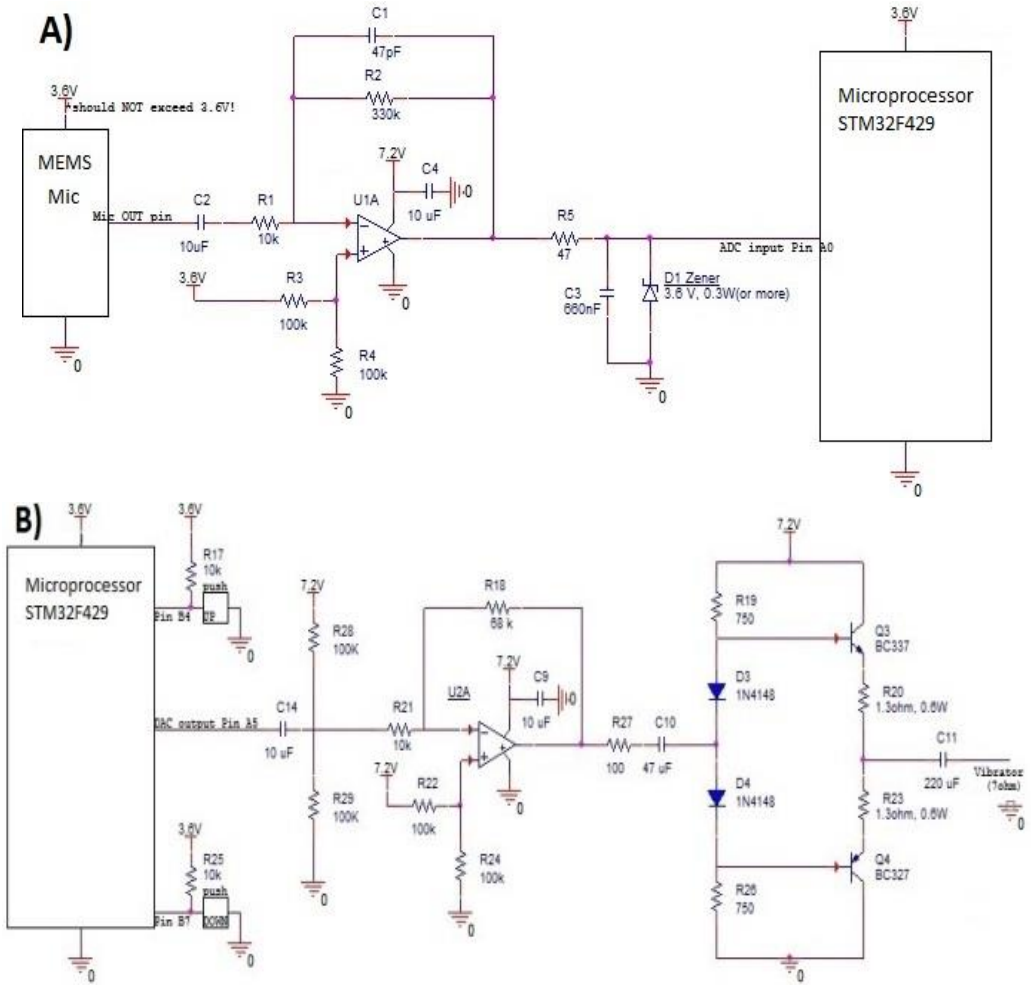

Fig. 2: A) The input analog pre-processing stage. B) The output analog power stage.

C1 is chosen 47 pF so that a low-pass filter with 3-dB cutoff frequency at about 4 kHz is created according to (1) above. A second low pass filter is created by R5 and C3 with cutoff frequency at about 5 kHz. These two filters together achieve approximately 30 dB attenuation at the Nyquist rate (i.e. half of the sampling frequency) which is 12 kHz. This should be adequate for removing the undesired aliasing components [11] in the sampled signal.

2.3 Digital Signal Processing

Fig. 3 depicts the digital signal processing implementation inside the STM32F429 microprocessor. The captured signal processed by the analogue input stage (Fig. 2(A)) is sampled by the microprocessor's 12-bit internal ADC. The timer of the ADC is set so that sampling occurs at 24 kHz. Two buffers (B1 and B2 in Fig. 3) are used. Each audio buffer is 512

ISSN: 2456-1851

Volume: 04, Issue: 05 "September-October 2019"

samples long, which corresponds to 21.3ms in time. When the first buffer (B1) is filled, an interrupt is generated. The buffer is then processed by the CPU. While the buffer is being processed, the ADC mechanism is ongoing independently and new samples are prepared and written into the second buffer (B2) to be fetched and processed by the CPU in the next cycle. This procedure continues and the data are filled in B1 and B2 and fetched by the CPU consecutively. This double buffering mechanism, empowered by the DMA, guarantees a continuous real-time flow of the data from microphone as long as the CPU processing time per buffer does not become longer than a buffer size itself (21.3ms) which is the case here because the IDE tools show that the entire processing of a single buffer (512 samples) takes less than 1ms.

A simple noise-management is implemented which calculates the root mean square (RMS) energy of each buffer. If the value is lower than a threshold, which corresponds to the RMS associated with a 40 dB SPL sinusoid in the input, the content of the buffer is discarded and filled with zeros. Although this noise-management algorithm is simple, it significantly reduces the battery consumption that is due to unwanted low-amplitude sound fluctuations which still drive the vibrator unnecessarily.

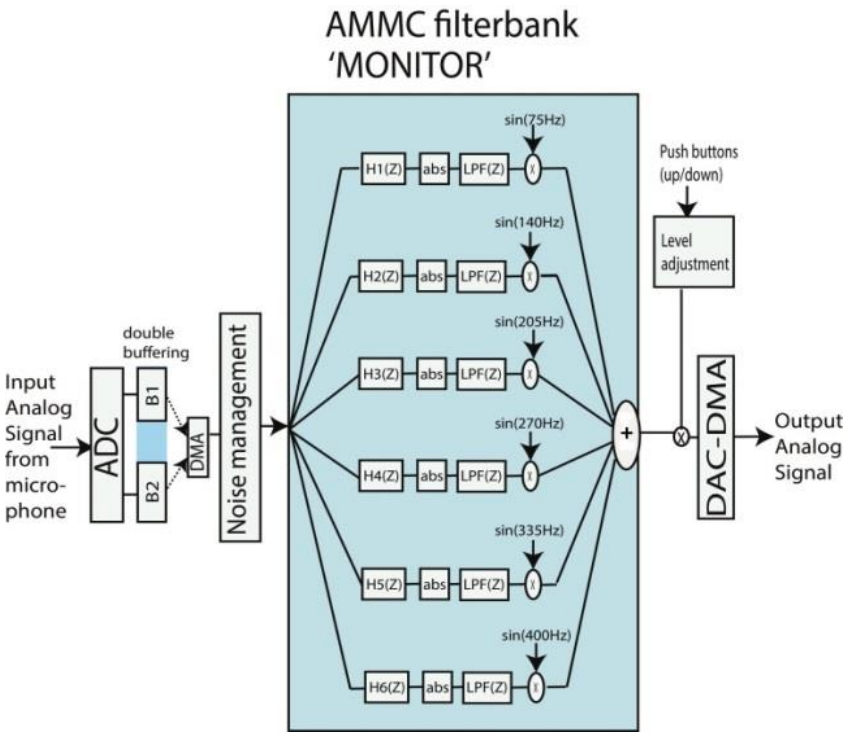

Fig. 3: The digital signal processing implementation block diagram.

ISSN: 2456-1851

Volume: 04, Issue: 05 "September-October 2019"

The six band-pass FIR filters (H1 to H6 in Fig.3) and the LPF are implemented using the standard filter library ("*filter.h*") written for ARM Cortex-M4 with DSP instructions. Each channel is modulated by multiplying the samples with a sinusoid at a specific frequency, as seen in Fig. 3, and the results of all 6 channels are summed and multiplied by a scaling factor that is adjusted by the user via pushing the up and down buttons. The result is delivered to the DMA unit that routes the buffer to one of the microprocessor's 12-bit internal DAC modules. The DMA unit allows the CPU to process the next buffer while the DAC is busy converting and playing the current buffer.

MONITOR filterbank algorithm (Fig. 1 (A)) was also simulated in MATLAB for various input sounds and the simulation results were compared with the output of the presented DSP implementation to verify that they both yield a similar waveform.

2.4 Analog Output Power Stage

The output from the DAC is buffered and amplified by UA2 operational amplifier in an inverting configuration with the gain set by R18/R23 ratio which is for matching the impedance of the DAC port with that of the succeeding bipolar junction transistor (BJT) amplifier. As seen in Fig. 2(B), the amplifier stage consists of a PNP BJT (i.e. BC327) and a NPN BJT (i.e. BC337) that are put together in a class AB (i.e. push-pull) configuration. This push-pull amplifier stage delivers about 0.5W power to the 7-ohm load (from the vibrator component) when the input signal is 3.6V peak to peak, corresponding to a 94 dB SPL sinusoid.

3. RESULTS

Fig. 4(A) shows the output signal to the vibrator (blue line), measured by an oscilloscope, in response to a 1 KHz input tone at 94 dB SPL. According to the MONITOR algorithm, this input signal is filtered by H3 and is then amplitude-modulated by a 205 Hz sinusoid. As a result, the output signal, seen in Fig. 4(A) consists of a slowly-varying carrier frequency component (at 205 Hz) which is carrying a fast-varying component that conveys the fine temporal structure of the sound. The black line shows the output of the MATLAB simulation for the same input and depicts a close match with the measured output (blue line).

ISSN: 2456-1851

Volume: 04, Issue: 05 "September-October 2019"

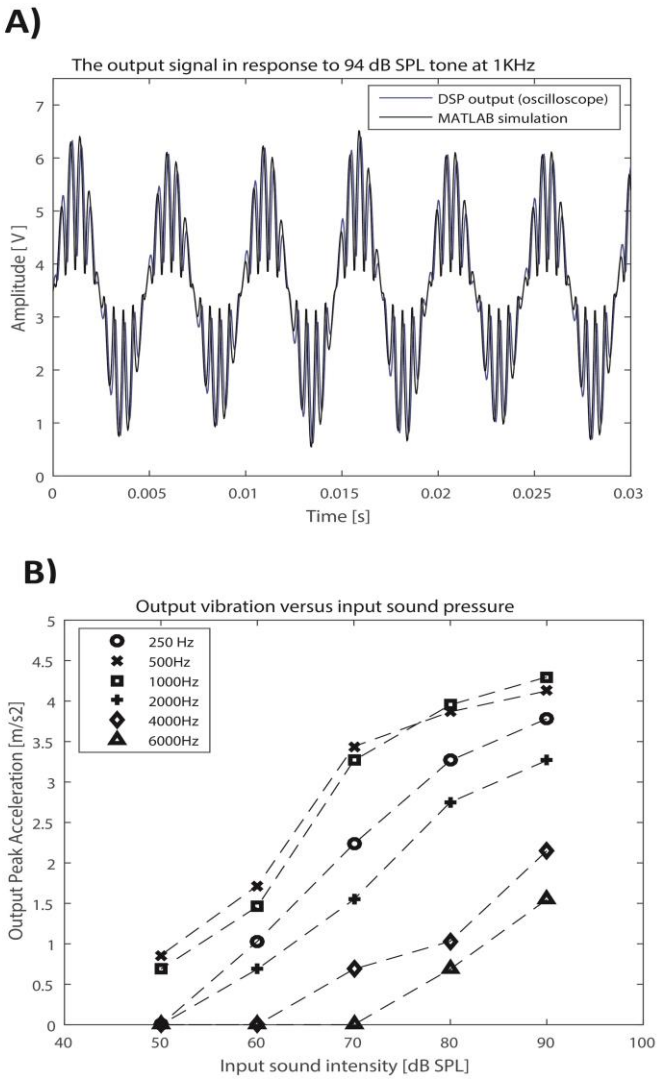

Fig. 4: A) The output signal waveform. B) The mechanical acceleration produced by the vibrator probe in response to input tones at 0.25, 0.5, 1, 2, 4, and 6 kHz and at intensities from 50 to 90 dB SPL.

The output signal, shown in Fig. 4(A), is biased at 3.6 V DC and appears to be 6.2V peak to peak. The reason why this value is 1V below the supply voltage at 7.2V is that there is around 1V voltage drop over R20 and R23, which are meant for temperature stability of the output power stage.

The accelerations produced by the vibrator from the waveform shown in Fig. 4(A) were measured using the Brüel & Kjær type 4371 accelerometer. This charge accelerometer shows an AC-coupled signal with a 25 mV peak value. Brüel & Kjær type 4371 is calibrated to generate a

ISSN: 2456-1851

Volume: 04, Issue: 05 "September-October 2019"

57mV peak in response to gravity (i.e., 9.8 [m/s2]). Therefore, the measured 25 mV peak value corresponds to 4.3 [m/s2]. According to Oey and Miller measurements [7] with similar vibrotactile probe, the fingertip skin vibratory sensation threshold at 200 Hz is around 0.1 [m/s2]. Therefore, the resulting vibration is more than 40 folds over the threshold. Basic user tests showed that these vibrations (generating 4.3 [m/s2] of mechanical acceleration) are very clearly sensed on the wrist as well.

Accelerations were similarly measured at the output of the system in response to input tones at 0.25, 0.5, 1, 2, 4, and 6 kHz and intensities from 50 to 90 dB SPL, covering the majority of the dynamic range (i.e., 40 to 94 dB SPL), and results are reported in Table I below. Fig. 4(B) illustrates the acceleration values in Table I as a function of sound intensity at different frequencies. Fig. 4(B) shows that the system codes a broad frequency range of input sinusoid from 0.25 to 6 kHz and that the input/output relationship of these curves is relatively linear at low intensities but becomes compressive at high intensities.

Table I: The measured vibration generated by the vibrator probe at the output. The table shows the accelerations (in [m/s2]) and the corresponding peak voltages, measured in [mV], in parentheses.

	0.25 kHz	**0.5 kHz**	**1 kHz**	**2 kHz**	**4 kHz**	**6 kHz**
90dB SPL	3.78 (22)	4.12 (24)	4.3 (25)	3.27 (19)	2.14 (12.5)	1.55 (9)
80dB SPL	3.27 (19)	3.9 (22.5)	3.95 (23)	2.75 (16)	1.03 (6)	0.69 (4)
70dB SPL	2.2 (13)	3.44 (20)	3.27 (19)	1.55 (9)	0.69 (4)	0
60dB SPL	1.03 (6)	1.72 (10)	1.55 (9)	0.69 (4)	0	0
50dB SPL	0	0.86 (5)	0.67 (4)	0	0	0

3.1 Frequency Range, Audio Latency, and Current Consumption Metrics

The lower end of the frequency range of the system is determined by C11 in Fig. 2(B) which is set to filter out the DC and very-low frequency components lower than 0.1 kHz. On the other hand, Table I and Fig. 4(B) indicate that frequencies as high as up to 6 kHz are coded by the

ISSN: 2456-1851

Volume: 04, Issue: 05 "September-October 2019"

system. The achieved frequency range (0.1 to 6 kHz) of the presented implementation is much broader than that of Sentiphone MiniVib4 [3] which was designed to code input sounds between 0.5 and 2.3 kHz only.

The DSP was coded to process the incoming sounds in buffers of 512 samples, each corresponding to 21.3ms at the sample rate used here (i.e. 24 kHz). The information arriving at the DAC is lagged from the ADC by the time equivalent of one single buffer (21.3ms) plus the time needed for the CPU to process the buffer (about 1ms). In other words, the total signal input-to-output propagation latency is less than 23ms.

The IDE tools show that the STM32F4 microprocessor constantly consumes about 48 mA while, according to the direct reading on the power supply, the analog circuits (Fig. 2(A) and Fig. 3(B)) draw around 11 mA in silence (no load). Therefore, the total no-load current consumption of the system is about 59 mA. When a 94 dB SPL sinusoid at 1 kHz was played (full load), the total current consumption increased to about 120 mA. The reported current consumption values can be reduced by about 40 mA, if the ultra-low-power version (STM32L4) of this microprocessor is used, instead.

4. DISCUSSION

Table I and Fig. 4(B) suggest that although all six filters contribute to the output, their contributions are different and that the vibrator generates the highest vibrations in response to 500 and 1000 Hz input tones. These two tones are related to the second and third channels of the algorithm, which are filtered by H2 and H3 that process low frequencies (300-600 Hz) and mid-range frequencies (600-1200 Hz). These two filters are modulated by sinusoids at 140 and 205 Hz, respectively. This is deliberately consistent with the fact that the skin's mechanoreceptors are most sensitive at around 200 Hz [6], [7].

Furthermore, the contribution of H1 (0-300 Hz), H4 (1200-2400Hz), and H5 (2400-5000 Hz) are also substantial. However, the 6th channel (H6) that filters very-high frequency components (5000 – 8000 Hz) showed minimal contribution to the output, solely at high intensities (80 and 90 dB SPL). This suggests that, if technical limitations require a smaller code, the 6th channel could be removed from the algorithm with minimal difference in the overall performance of the system.

4.1 The Novelty of the Presented Implementation

This paper presents a prototype that runs on 7.2V (two standard 3.6V batteries in series) and relies on a small DSP core and a rather simple analog circuitry with relatively low power

ISSN: 2456-1851

Volume: 04, Issue: 05 "September-October 2019"

consumption and low latency. These factors make this design suitable for producing a wearable battery-driven medical device. The results showed that the presented system codes a much broader frequency range of input sounds (0.1 to 6 kHz) than the existing Sentiphone MiniVib4 solution [3] (0.5 to 2.3 kHz).

Ranjbar and Stenstörm [8] implemented the MONITOR algorithm as a mobile application on an HTC Android cellphone. The major drawback of their mobile-based implementation was that it required the user to wear the cellphone, the vibrator, and an external amplifier as separate modules wired together. This negatively affected its practical usability as a wearable medical device. Moreover, the loose wiring between the standalone modules could even lead to safety hazards for the user. Additionally, since the phone uses the Android operative system, the audio latency can become an issue. The Android audio architecture consists of several layers [12] and it can take over 300ms for the audio signals captured by the microphone to propagate to the JAVA application layer where the algorithm is eventually applied and then propagate down to the external output amplifier. This long round-trip latency (300ms) could undermine and violate the real-time concept of the implementation. This is in contrast with the presented DSP-based implementation where the total latency from input (microphone) to output (vibrator) is merely 23ms.

5. FUTURE WORKS

This paper presented a real-time implementation of the MONITOR algorithm on an STM32F429 ARM Cortex-M4 DSP. The presented system was primarily designed and implemented for aiding the users to monitor and identify surrounding sounds such as door bells, alarms, and sudden incidents. However, helping post-lingual individuals with residual vision, who are capable of lip-reading, to improve their speech perception is also an important goal. Ranjbar and Stenstörm [8] tested their mobile-based prototype of MONITOR on four individuals with deafblindness. They achieved promising results indicating the potentials of this algorithm in aiding the severely hearing-impaired individuals, as well as deafblindness. Even so, comprehensive in-field tests are necessary to verify the feasibility of the presented solution in addressing the real-life needs of the users in realistic situations (such as in [5]) and to help explore the road map for future improvements.

6. ACKNOWLEDGMENT

This work was funded by the Swedish innovation office, Örebro University Holding AB and Promobilia.

ISSN: 2456-1851

Volume: 04, Issue: 05 "September-October 2019"

REFERENCES

E. Borg, J. Roenberg, L. Neoveius, and K. Moeller, "Monitoring environmental events: problems, strategies and sensory compensation," ISAC00 Conference, 2000.

G. Plant, and K. E. Spens, *Profound deafness and speech communication*, Whurr Publishers Limited., UK, 1995.

H. Traunmueüller, "The Sentiphone: A tactual speech communication aid," J. Commun Disord. 13(3), pp. 183–93, 1980.

K. E. Spens, and G. Plant, "A tactual 'hearing' aid for the deaf," STL-QPSR. 24(1), pp. 52-56, 1983.

P. Ranjbar, E. Borg, L. Philipson, and D. Stranneby, "Auditive identification of signal-processed environmental sounds: Monitoring the environment," Int. J. of Audiol. 47, pp. 724-736, 2008.

A. B. Vallbo, and R. S. Johansson, "Properties of cutaneous mehchanoreceptors in the human hand related to touch sensation," Human Neurobiol. 3(1), pp. 3-14, 1984.

H. Oey, and V. Mellert, "Vibration thresholds and equal vibration levels at the human fingertip and palm," ICA, pp. 1-4, 2004.

P. Ranjabr, and I. Stenstörm, "A vibrotactile aid for environmental perception: A field evaluation by four people with severe hearing and vision impairment," The Scientific World Journal (V.2013), pp 1-11, 2013.

STMicroelectronics, "STM32F4 Series," link: https://www.st.com/en/microcontrollers/stm32f4-series.html?querycriteria=productId=SS1577 (last viewed 26/10/2018).

A. Osborne, An Introduction to Microcomputers: Volume 1: Basic Concepts (2nd ed.), Osborne McGraw Hill, UK, pp. 5–93, 1983.

A. V. Openheim, L. S. Willsky, and S. H. Nawab, Signals and Systems (2nd ed.), Pearson Education Limited, USA, pp. 427-519, 2014.

Google Android team, "Online documentation: Audio architecture in Android," link: https://source.android.com/devices/audio/ (last viewed 5/2/2019).

